Changes in temperature alter susceptibility to a virus following a host shift

Short title: Influence of temperature on virus host shifts

Katherine E. Roberts[1*], Jarrod D. Hadfield[2], Manmohan D. Sharma[1] and Ben Longdon[1]

[1] Biosciences, College of Life & Environmental Sciences, University of Exeter, Penryn Campus, Penryn, Cornwall, TR10 9FE, UK

[2] Institute of Evolutionary Biology, School of Biological Sciences, The University of Edinburgh, Ashworth Laboratories, The King's Buildings, Charlotte Auerbach Road, Edinburgh, EH9 3FL, UK

* Corresponding author: k.roberts@exeter.ac.uk

Abstract

Host shifts – where a pathogen jumps between different host species – are an important source of emerging infectious disease. With ongoing climate change there is an increasing need to understand the effect changes in temperature may have on emerging infectious disease. We investigated whether species' susceptibilities change with temperature and ask if susceptibility is greatest at different temperatures in different species. We infected 45 species of *Drosophilidae* with an RNA virus and measured how viral load changes with temperature. We

found the host phylogeny explained a large proportion of the variation in viral load at each temperature, with strong phylogenetic correlations between viral loads across temperature. The variance in viral load increased with temperature, whilst the mean viral load did not, such that as temperature increased the most susceptible species become more susceptible, and the least susceptible less so. We found no significant relationship between a species' susceptibility across temperatures and proxies for thermal optima; critical thermal maximum and minimum or basal metabolic rate. These results suggest that whilst the rank order of species susceptibilities can remain the same with changes in temperature, the likelihood of host shifts into a given species may increase or decrease.

Author Summary

Emerging infectious diseases are often the result of a host shift, where a pathogen jumps from one host species into another. Understanding the factors underlying host shifts is a major goal for infectious disease researchers. This effort has been further complicated by the fact that host-parasite interactions are now taking place in a period of unprecedented global climatic warming. Here, we ask how host shifts are affected by temperature by carrying out experimental infections using an RNA virus across a wide range of related species, at three different temperatures. We find that as temperature increases the most susceptible species become more susceptible, and the least susceptible less so. This has important consequences for our understanding of host shift events in a changing climate, and suggests that temperature changes may affect the likelihood of a host shift into certain species.

48

49 Introduction

50 Temperature is arguably the most important abiotic factor that affects all
51 organisms, having both indirect and direct effects on physiology and life history
52 traits [1–3]. There is much to be learned about the impact of climate change on
53 infectious diseases [1,4,5]. Changes in temperature can impact both host and
54 parasite biology, leading to complex and difficult to predict outcomes [2,6].

55

56 Host shifts, where a parasite from one host species invades and establishes in a
57 novel host species, are an important source of emerging infectious disease [7].
58 Some of the most deadly outbreaks of infectious diseases in humans including
59 Ebola virus, HIV and SARS coronavirus have been linked to a host switch event [8–
60 11] and many others have direct animal vectors or reservoirs (e.g. Dengue and
61 Chikungunya viruses) [12,13]. The potential for novel host shifts may increase
62 with changing temperatures due to fluctuations in host and/or parasite fitness, or
63 changes in species distributions and abundances [14,15]. Distribution changes
64 may lead to new species assemblages, causing novel contacts between parasites
65 and potential hosts [16–18].

66

67 Susceptibility to infection is known to vary with temperature due to within
68 individual physiological changes in factors such as the host immune response,
69 metabolic rate or behavioural adaptations [19–22]. Thermally stressed hosts may
70 face a trade-off between the resource investment needed to launch an immune
71 response versus that needed for thermoregulation, or behavioural adaptations to
72 withstand sub-optimal temperatures [23–26]. Temperature shifts could also cause

73 asymmetrical or divergent effects on host and parasite traits [27]. For example,
74 changes in temperature may allow differential production and survival of parasite
75 transmission stages, and changes in replication rates, generation times, infectivity
76 and virulence [28–30].
77
78 Host shifts have been shown to be more likely to occur between closely related
79 species [31–33], but independently of this distance effect, clades of closely related
80 hosts show similar levels of susceptibility [34,35]. Thermal tolerances – like virus
81 susceptibility – are known to vary across species, with groups of closely related
82 species having similar thermal limits, with a large proportion of the variation in
83 these traits being explained by the phylogeny [36–39]. Previous studies on host
84 shifts have assayed the susceptibility of species at a single temperature
85 [32,34,35,40]. However, if the host phylogeny also explains much of the variation in
86 thermal tolerance, then phylogenetic patterns in virus susceptibility could be due
87 to differences between species' optima and the chosen assay temperatures.
88 Therefore, for experiments carried out at a single temperature, phylogenetic signal
89 in thermal tolerance may translate into phylogenetic signal in thermal stress. Any
90 apparent phylogenetic signal in susceptibility could potentially be due to the effects
91 of thermal stress, and may not hold true if each species was to be assayed at its
92 optimal temperature.
93
94 Here, we have asked how species susceptibilities change at different temperatures
95 and whether susceptibility is greatest at different temperatures in different species.
96 We infected 45 species of *Drosophilidae* with Drosophila C Virus (DCV;
97 Dicistroviridae) at three different temperatures and measured how viral load

98 changes with temperature. We also examine how proxies for thermal optima and
99 cellular function (thermal tolerances and basal metabolic rate) relate to virus
100 susceptibility across temperatures [37–39]. DCV is a positive sense RNA virus in
101 the family *Discistroviridae* that was isolated from *Drosophila melanogaster* and
102 naturally infects several species of Drosophilidae in the wild [41–43]. DCV infected
103 flies show reduced metabolic rate and activity levels, develop an intestinal
104 obstruction, reduced hemolymph pH and decreased survival [44–47]. This work
105 examines how temperature can influence the outcomes of host shifts, and looks at
106 some of the potential underlying causes.
107

108 # Methods

109 ## Experimental infections

110 We used Drosophila C virus (DCV) clone B6A, which is derived from an isolate
111 collected in Charolles, France [48]. The virus was prepared as described previously
112 [49]; briefly DCV was grown in Schneider's Drosophila line 2 cells and the Tissue
113 Culture Infective Dose 50 ($TCID_{50}$) per ml was calculated using the Reed-Muench
114 end-point method [50].
115

116 Flies were obtained from laboratory stocks of 45 different species. All stocks were
117 maintained in multi generation populations, in Drosophila stock bottles (Dutscher
118 Scientific) on 50ml of their respective food medium at 22°C and 70% relative
119 humidity with a 12 hour light-dark cycle (see table S1 for rearing conditions for
120 each species). Each day, two vials of 0-1 day old male flies were randomly assigned
121 to one of three potential temperature regimes; low, medium or high (17°C, 22°C
122 and 27 °C respectively) at 70% relative humidity. Flies were tipped onto fresh vials

of food after 3 days, and after 5 days of acclimatisation at the experimental temperature were infected with DCV. Flies were anesthetized on CO_2 and inoculated using a 0.0125 mm diameter stainless steel needle that was bent to a right angle ~0.25mm from the end (Fine Science Tools, CA, USA). The bent tip of the needle was dipped into the DCV solution ($TCID_{50}$ = 6.32×10^9) and pricked into the pleural suture on the thorax of the flies. One vial of inoculated flies was immediately snap frozen in liquid nitrogen to provide a time point zero sample as a reference to control for relative viral dose. The second vial of flies were placed onto a new vial of fresh cornmeal food and returned to their experimental temperature. After 2 days (+/- 1 hour) flies were snap frozen in liquid nitrogen, this time point was chosen based on pilot data as infected flies showed little mortality at 2 days post infection, and viral load plateaus from day 2 at 22°C. Temperatures were rotated across incubators in each block to control for incubator effects. All frozen flies were homogenised in a bead homogeniser for 30 seconds (Bead Ruptor 24; Omni international, Georgia, USA) in Trizol reagent (Invitrogen) and stored at -80°C for later RNA extractions.

These collections and inoculations were carried out over three replicate blocks, with each block being completed over consecutive days. The order that the fly species were infected was randomized each day. We aimed for each block to contain a day 0 and day 2 replicate for each species, at each temperature treatment (45 species × 3 temperatures × 3 experimental blocks). In total we quantified viral load in 12,827 flies, with a mean of 17.1 flies per replicate (range across species = 4-27). Of the 45 species, 44 had 6 biological replicates and one species had 5 biological replicates.

148

149 **Measuring the change in viral load**

150 The change in RNA viral load was measured using qRT-PCR. Total RNA was
151 extracted from the Trizol homogenised flies, reverse-transcribed with Promega
152 GoScript reverse transcriptase (Promega) and random hexamer primers. Viral RNA
153 load was expressed relative to the endogenous control housekeeping gene *RpL32*
154 (*RP49*). *RpL32* primers were designed to match the homologous sequence in each
155 species and crossed an intron-exon boundary so will only amplify mRNA [34]. The
156 primers in *D. melanogaster* were *RpL32* qRT-PCR F (5'-
157 TGCTAAGCTGTCGCACAAATGG -3') and *RpL32* qRT-PCR R (5'-
158 TGCGCTTGTTCGATCCGTAAC -3'). DCV primers were 599F (5'-
159 GACACTGCCTTTGATTAG-3') and 733R (5'CCCTCTGGGAACTAAATG-3') as
160 previously described [35]. Two qRT-PCR reactions (technical replicates) were
161 carried out per sample with both the viral and endogenous control primers, with
162 replicates distributed across plates in a randomised block design.

163

164 qRT-PCR was performed on an Applied Biosystems StepOnePlus system using
165 Sensifast Hi-Rox Sybr kit (Bioline) with the following PCR cycle: 95°C for 2min
166 followed by 40 cycles of: 95°C for 5 sec followed by 60°C for 30 sec. Each qRT-PCR
167 plate contained four standard samples. A linear model was used to correct the cycle
168 threshold (Ct) values for differences between qRT-PCR plates. Any samples where
169 the two technical replicates had cycle threshold (Ct) values more than 2 cycles
170 apart after the plate correction were repeated. To estimate the change in viral load,
171 we first calculated *ΔCt* as the difference between the cycle thresholds of the DCV
172 qRT-PCR and the *RpL32* endogenous control. The viral load of day 2 flies relative to

day 0 flies was then calculated as $2^{-\Delta\Delta Ct}$, where $\Delta\Delta Ct = \Delta Ct_{day0} - \Delta Ct_{day2}$, where ΔCt_{day0} and ΔCt_{day2} are a pair of ΔCt values from a day 0 biological replicate and a day 2 biological replicate for a particular species. Calculating the change in viral load without the use of the endogenous control gene (*RpL32*) gave equivalent results (Spearman's correlation between viral load calculated with and without endogenous control: $\rho = 0.97$, $P < 0.005$)

Critical Thermal Maximum and Minimum Assays

We carried out two assays to measure the thermal tolerances of species; a cold resistance measure to determine critical thermal minimum (CT_{min}) under gradual cooling, and a heat resistance measure through gradual heating to determine critical thermal maximum (CT_{max}). 0-1 day old males were collected and placed onto fresh un-yeasted cornmeal food vials. Flies were kept for 5 days at 22°C and 70% relative humidity and tipped onto fresh food every 2 days. In both assays individual flies were placed in 4 ml glass vials (ST5012, Ampulla, UK) and exposed to temperature change through submersion in a liquid filled glass tank (see supplementary material and methods for description of apparatus). For CT_{max} the tank was filled with water and for CT_{min} a mixture of water and ethylene glycol (50:50 by volume) was used to prevent freezing and maintain a constant cooling gradient. Five biological replicates were carried out for each species for both CT_{max} and CT_{min}. Temperature was controlled using a heated/cooled circulator (TXF200, Grant Instruments, Cambridgeshire, UK) submerged in the tank and set to change temperatures at a rate of 0.1 °C/min, always starting from 22°C (the rearing temperature for stock populations). Flies were monitored continually throughout the assay and the temperature of knock down was ascertained by a disturbance

198 method, whereby a fly was scored as completely paralysed if on gentle tapping of
199 the vial wall the fly did not move any of its body parts.
200
201 **Measuring Metabolic Rate**
202 To examine how cellular function changes with temperature, we estimated the
203 resting metabolic rate of each species at 17°C, 22°C and 27 °C. Following the same
204 methods as the viral inoculation assay, groups of 10, 0-1 day old male flies from 44
205 species were acclimatised at the three experimental temperatures for 5 days (*D.*
206 *pseudobscura* was excluded as not enough individuals could be obtained from
207 stocks for sufficient replication). Every 2 days flies were tipped onto fresh vials of
208 cornmeal food. This was repeated in three blocks in order to get three repeat
209 measures of metabolic rate for each of the species, at each of the three
210 experimental temperatures. Flies were collected in a randomly assigned order
211 across the three blocks
212
213 Closed system respirometry was used to measure the rate of CO_2 production
214 (VCO_2) as a proxy for metabolic rate [51]. Flies were held in $10ml^{-3}$ airtight plastic
215 chambers constructed from Bev-A-Line V Tubing (Cole-Parmer Instrument
216 Company, UK). All measures were carried out during the day inside a temperature
217 controlled incubator, with constant light, that was set to each of the experimental
218 temperatures that the flies had been acclimatised to. The set up followed that of
219 Okada *et al.* (2011)[52]. Compressed air of a known concentration of oxygen and
220 nitrogen (21% O_2:79% N_2) was scrubbed of any CO_2 and water (with Ascarite II &
221 Magnesium Perchlorate respectively) and pumped through a Sable Systems RM8
222 eight-channel multiplexer (Las Vegas, NV, USA) at 100 ml/min^{-1} (±1%) into the

metabolic chambers housing the groups of 10 flies. The first chamber was left empty as a reference cell, to acquire a baseline reading for all subsequent chambers at the start and end of each set of runs, therefore seven groups of flies were assayed in each run. Air was flushed into each chamber for 2 minutes, before reading the previous chamber. Readings were taken every second for 10 minutes by feeding the exiting air through a LiCor LI-7000 infrared gas analyser (Lincoln, NE, USA). Carbon dioxide production was measured using a Sable Systems UI2 analog–digital interface for acquisition, connected to a computer running Sable Systems Expedata software (v1.8.2) [53]. The metabolic rate was calculated from the entire 10-minute recording period, by taking the CO_2 reading of the ex-current gas from the chamber containing the flies and subtracting the CO_2 measure of the incurrent gas entering the chamber. These values were also corrected for drift away from the baseline reading of the empty chamber. Volume of CO_2 was calculated as $VCO_2 = FR (Fe\ CO_2 – Fi\ CO_2) / (1-Fi\ CO_2)$. Where FR is the flow rate into the system ($100ml/min^{-1}$), Fe CO_2 is the concentration of CO_2 exiting and Fi CO_2 is the concentration CO_2 entering the respirometer. Species were randomly assigned across the respiration chambers and the order in which flies were assayed in (chamber order) was corrected for statistically (see below).

Body Size

To check for any potential effect of body size differences between species, wing length was measured as a proxy for body size [54]. A mean of 26 (range 20-30) males of each species were collected and immediately stored in ethanol during the collections for the viral load assay. Subsequently, wings were removed and photographed under a dissecting microscope. Using ImageJ software (version 1.48)

248 the length of the IV longitudinal vein from the tip of the proximal segment to where
249 the distal segment joins vein V was recorded, and the mean taken for each species.
250
251 **Host phylogeny**
252 The host phylogeny was inferred as described in Longdon *et al* (2015) [35], using
253 the *28S, Adh, Amyrel, COI, COII, RpL32* and *SOD* genes. Briefly, any publicly available
254 sequences were downloaded from Genbank, and any not available we attempted to
255 sanger sequence [34]. In total we had *RpL32* sequences for all 45 species, 41 for
256 *28s*, 43 for *Adh*, 29 for *Amyrel,* 38 for *COI*, 43 for *COII* and 25 for *SOD* (see Figshare
257 10.6084/m9.figshare.6653192 for full details). The sequences of each gene were
258 aligned in Geneious (version 9.1.8, [55]) using the global alignment setting, with
259 free end gaps and a cost matrix of 70% similarity. The phylogeny was constructed
260 using the BEAST program (version 1.8.4,[56]). Genes were partitioned into three
261 groups each with their own molecular clock models. The three partitions were:
262 mitochondrial (*COI*, *COII*); ribosomal (*28S*); and nuclear (*Adh*, *SOD*, *Amyrel*, *RpL32*).
263 A random starting tree was used, with a relaxed uncorrelated lognormal molecular
264 clock. Each of the partitions used a HKY substitution model with a gamma
265 distribution of rate variation with 4 categories and estimated base frequencies.
266 Additionally, the mitochondrial and nuclear data sets were partitioned into codon
267 positions 1+2 and 3, with unlinked substitution rates and base frequencies across
268 codon positions. The tree-shape prior was set to a birth-death process. The BEAST
269 analysis was run twice to ensure convergence for 1000 million MCMC generations
270 sampled every 10000 steps. The MCMC process was examined using the program
271 Tracer (version 1.6, [57]) to ensure convergence and adequate sampling, and the
272 constructed tree was then visualised using FigTree (version 1.4.3, [58]).

Statistical analysis

All data were analysed using phylogenetic mixed models to look at the effects of host relatedness on viral load across temperature. We fitted all models using a Bayesian approach in the R package MCMCglmm [59,60]. We ran trivariate models with viral load at each of the three temperatures as the response variable similar to that outlined in Longdon *et al.* (2011) [34]. The models took the form:

$$y_{hit} = \beta_{1:t} + bmr_h \cdot \beta_2 + wingsize_h \cdot \beta_3 + CTmin_h.\beta_4 + CTmax_h \cdot \beta_5 + u_{p:ht} + e_{hit}$$

Where y is the change in viral load of the i^{th} biological replicate of host species h, for temperature t (high, medium or low). β are the fixed effects, with β_1 being the intercepts for each temperature, β_2 being the effect of basal metabolic rate, β_3 the effect of wing size, and β_4 and β_5 the effects of the critical thermal maximum (CT_{max}) and minimum (CT_{min}) respectively. u_p are the random phylogenetic species effects and e the model residuals. We also ran models that included a non-phylogenetic random species effect ($u_{np:ht}$) to allow us to estimate the proportion of variation explained by the host phylogeny [34,35,61]. We do not use this term in the main model as we struggled to separate the phylogenetic and non-phylogenetic terms. Our main model therefore assumes a Brownian motion model of evolution [62]. The random effects and the residuals are assumed to be multivariate normal with a zero mean and a covariance structure $\mathbf{V_p} \otimes \mathbf{A}$ for the phylogenetic affects and $\mathbf{V_e} \otimes \mathbf{I}$ for the residuals. **A** is the phylogenetic relatedness matrix, **I** is an identity matrix and the **V** are 3×3 (co)variance matrices describing the (co)variances between viral

297 titre at different temperatures. The phylogenetic covariance matrix, $\mathbf{V_p}$, describes
298 the inter-specific variances in each trait and the inter-specific covariances between
299 them. The residual covariance matrix, $\mathbf{V_e}$, describes the within-species variance that
300 can be both due to real within-species effects and measurement or experimental
301 errors. The off-diagonal elements of $\mathbf{V_e}$ (the covariances) are not estimable because
302 no vial has been subject to multiple temperatures and so were set to zero. We
303 excluded *D. pseudoobscura* from the full model as data for BMR was not collected,
304 but included it in models that did not include any fixed effects, which gave
305 equivalent results.
306
307 Diffuse independent normal priors were placed on the fixed effects (means of zero
308 and variances of 10^8). Parameter expanded priors were placed on the covariance
309 matrices resulting in scaled multivariate F distributions which have the property
310 that the marginal distributions for the variances are scaled (by 1000) $F_{1,1}$. The
311 exceptions were the residual variances for which an inverse-gamma prior was used
312 with shape and scale equal to 0.001. The MCMC chain was run for 130 million
313 iterations with a burn-in of 30 million iterations and a thinning interval of 100,000.
314 We confirmed the results were not sensitive to the choice of prior by also fitting
315 models with inverse-Wishart and flat priors for the variance covariance matrices
316 (described in [34]), which gave qualitatively similar results (data not shown). All
317 confidence intervals (CI's) reported are 95% highest posterior density intervals.
318
319 Using similar model structures we also ran a univariate model with BMR and a
320 bivariate model with CT_{min} and CT_{max} as the response variables to calculate how
321 much of the variation in these traits was explained by the host phylogeny. Both of

these models were also run with wing as a proxy for body size as this is known to influence thermal measures [51]. We observed significant levels of measurement error in the metabolic rate data; this was partially caused by respiratory chamber order during the assay. We corrected for this in two different ways. First, we fitted a linear model to the data to control for the effect of respiratory chamber number and then used this corrected data in all further models. We also used a measurement error model that controls for both respiratory chamber number effects and random error. Both of these models gave similar results although the measurement error model showed broad CIs suggesting the BMR data should be interpreted with caution. All datasets and R scripts with the model parameterisation are provided as supplementary materials.

Results

To investigate the effect of temperature on virus host shifts we quantified viral load in 12,827 flies from 45 species of Drosophilidae at three temperatures (Fig 1). DCV replicated in all host species, but viral load differed between species and temperatures (Fig 1). Species with similar viral loads cluster together on the phylogeny (Fig 2). Measurements were highly repeatable (Table 1), with a large proportion of the variance being explained by the inter-specific phylogenetic component (v_p), with little within species or measurement error (v_r) (Repeatability= $v_p/(v_p + v_r)$: Low = 0.90 (95% CI: 0.84, 0.95), Medium = 0.96 (95% CI: 0.93, 0.98), and High = 0.95, (95% CI: 0.89, 0.98)). We also calculated the proportion of between species variance that can be explained by the phylogeny as $v_p/(v_p+ v_s)$ [63], which is equivalent to Pagel's lambda or phylogenetic heritability [61,64]. We found the host phylogeny explains a large proportion of the inter-

specific variation in viral load across all three temperatures, although these estimates have broad confidence intervals due to the model struggling to separate the phylogenetic and non-phylogenetic components (Low = 0.77, 95% CI: 0.28, 0.99; Medium = 0.53, 95% CI: 0.31×10^{-5}, 0.85; High = 0.40, 95% CI: 0.99×10^{-5}, 0.74).

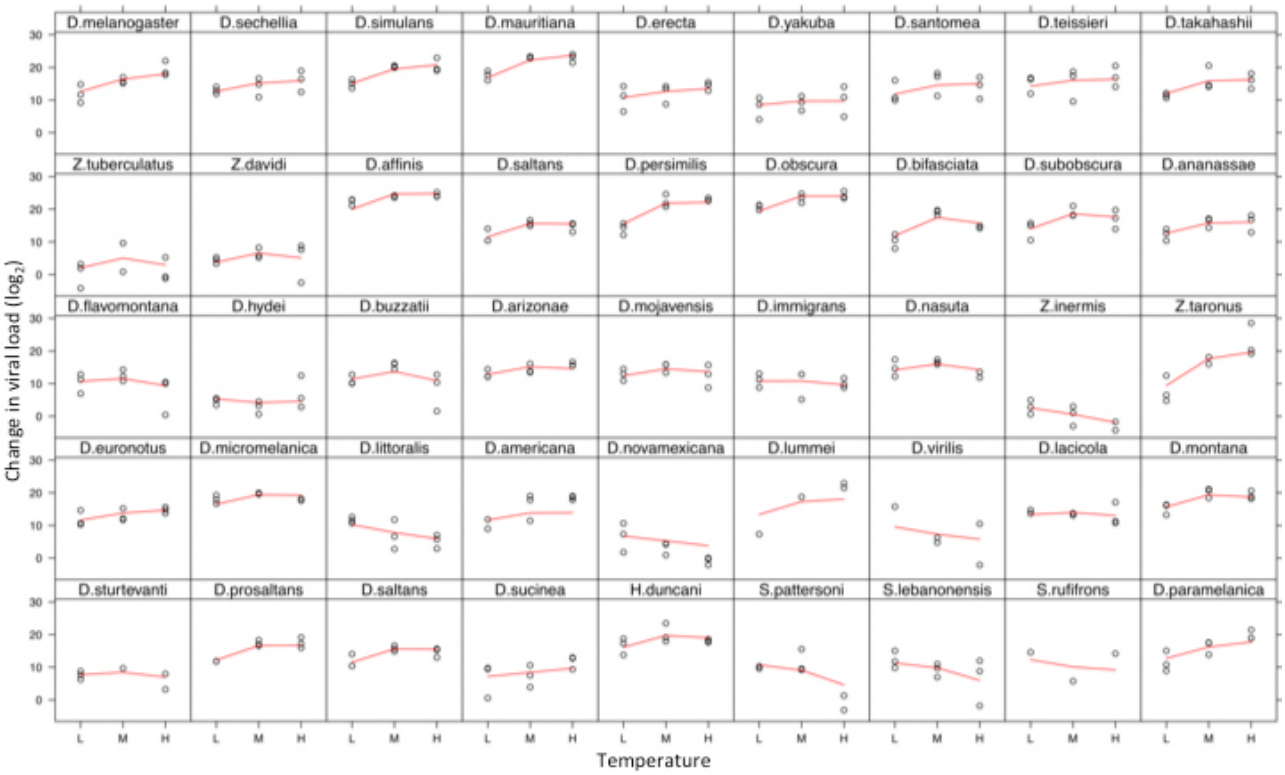

Fig 1. Change in viral load (log_2) for 45 *Drosophilidae* species across three temperatures (Low= 17°C, Medium=22°C and High=27°C). Individual points are for each replicate (change in viral load between day 0 and day 2 post infection), the red line is the predicted values from the phylogenetic mixed model. Panels are ordered by the tips on the phylogeny as in Fig 2.

To examine if species responded in the same or different way to changes in temperature we examined the relationships between susceptibilities across the different temperatures. We found strong positive phylogenetic correlations between viral loads across the three temperatures (Table 2). Our models showed that the variance in viral load increased with temperature, whilst the mean viral

load showed no such upward trend (Table 1), suggesting that the variance changes are not just due to scaling effects.

Table 1. Change in viral load with temperature.

Temperature	Intercepts		Between-species Variance (v_p)		Within-species Variance (v_r)	
	Mean	95% CIs	Mean	95% CIs	Mean	95% CIs
Low	11.9	9.5, 14.6	65.3	32.3, 110.3	6.9	4.8, 9.3
Medium	14.3	11.7, 17.1	172.2	90.2, 278.8	7.0	4.8, 9.2
High	13.5	10.8, 16.7	260.6	119.7, 413.7	12.8	8.9, 17.5

Intercepts are the temperature-specific intercepts when the other covariates (e.g. wing size) are set to their temperature specific means. They can be interpreted as the expected viral loads at the root of the phylogeny at each temperature. $\boldsymbol{v_p}$ is the variance in between-species effects, which are structured by the phylogeny, and $\boldsymbol{v_r}$ is the variance in within species effects attributable to between individual differences and measurement error.

Table 2. Interspecific correlations between viral loads at each temperature.

Temperatures	Interspecific Correlation	95% CIs
High-Low	0.89	0.77, 0.98
Medium-Low	0.92	0.90, 0.99
Medium-High	0.97	0.93, 0.99

The high correlations suggest the rank order of susceptibility of the species is not changing with increasing temperature. However, the change in variance suggests that although the reaction norms are not crossing they are diverging from each other as temperature increases i.e. the most susceptible species are becoming more susceptible with increasing temperature, and the least susceptible less so [65]. For

example, *D. obscura* and *D. affinis* are the most susceptible species at all three temperatures. The responses of individual species show that some species have increasing viral load as temperature increases (Fig 1, e.g. *Z. taronus*, *D. lummei*), whilst others decease (e.g. *D. littoralis, D. novamexicana*).

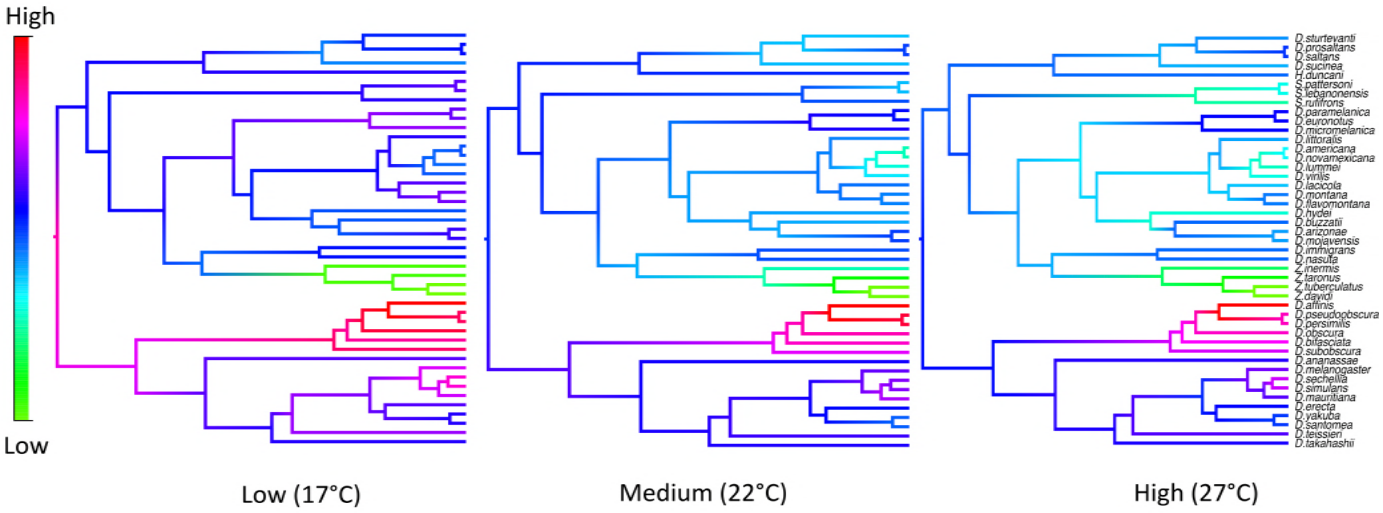

Fig 2. Ancestral state reconstructions to visualise the change in viral load across the host phylogeny at three temperatures. Ancestral states are plotted as colour gradients across the tree. The colour gradient represents the change in RNA viral load; red represents the highest and green the lowest viral load at that temperature. Ancestral states were estimated using a phylogenetic mixed model that partitioned the inter-specific variance into that explained by the host phylogeny under a Brownian model of evolution (v_p), and a species-specific variance component that is not explained by the phylogeny (v_s).

The changes we observe could be explained by the increase in temperature effectively increasing the rate at which successful infection is progressing (i.e. altering where in the course of infection we have sampled). However, this seems unlikely as at 2 days post infection at the medium temperature (22°C), viral load peaks and then plateaus [35]. Therefore, in those species where viral load increases

398 at higher temperatures the peak viral load itself must be increasing, rather than us
399 effectively sampling the same growth curve but at a later time point. Likewise, in
400 those species where viral load decreased at higher temperatures, viral load would
401 need to first increase and then decrease, which we do not observe in a time course
402 at 22°C [35]. To check whether this also holds at higher temperatures we carried
403 out a time course of infection in a subset of six of the experimental species at 27°C,
404 where we would expect the fastest transition between the rapid viral growth and
405 the plateau phase of infection to occur (S1 Fig), This allowed us to confirm that the
406 decreasing viral loads observed in some species at higher temperatures are not due
407 to general trend for viral loads to decline over longer periods of (metabolic) time.
408
409 We quantified the lower and upper thermal tolerances (CT_{min} and CT_{max}) across all
410 45 species with 3 replicates per species. Neither CT_{max} nor CT_{min} were found to be
411 significant predictors of viral load (CT_{min} -0.21, 95% CI: -0.79, 0.93, pMCMC = 0.95
412 and CT_{max} 0.31, 95% CI: -0.11, 0.74, pMCMC = 0.152). When treated as a response
413 in models we found the host phylogeny explained a large proportion of the
414 variation in thermal maximum (CT_{max} : 0.95, 95% CI: 0.84, 1) and thermal minima
415 (CT_{min} : 0.98, 95% CI: 0.92, 0.99, S2 Fig).
416
417 We also measured the basal metabolic rate of 1320 flies from 44 species, across the
418 three experimental temperatures, to examine how cellular function changes with
419 temperature. BMR was not found to be a significant predictor of viral load when
420 included as a fixed effect in our model (slope = 9.09, 95% CI = -10.13, 20.2689,
421 pMCMC = 0.548).
422

423 BMR increased with temperature across all species (mean BMR and SE: Low 0.64 ±
424 0.02, Medium 1.00 ± 0.04, High 1.2 ± 0.04 CO_2ml/min^{-1}, S3 Fig).
425 When BMR was analysed as the response in models, the phylogeny explained a
426 small amount of the between species variation (Low 0.19, 95% CI: 2×10^{-8}, 0.55,
427 Medium 0.10, 95% CI: 5×10^{-7}, 0.27, High 0.03, 95% CI: 8×10^{-9} - 0.13, S4 Fig)
428 indicating high within species variation or large measurement error. Consequently
429 the species/temperature mean BMRs used in the analysis of viral load will be
430 poorly estimated and so the effects of BMR will be underestimated with too narrow
431 credible intervals. To rectify this we ran a series of measurement error models, the
432 most conservative of which gave a slope of -9.8 but with very wide credible intervals
433 (-62.5, 42.6). Full details of these models are given in the Supplementary Materials.
434

435 ## Discussion

436 We found that susceptibilities of different species responded in different ways to
437 changes in temperature. The susceptibilities of different species showed either
438 increases or decreases at higher temperatures. There was a strong phylogenetic
439 correlation in viral load across the three experimental temperatures (Table 2).
440 However, the variance in viral load increased with temperature, whereas the mean
441 viral load did not show the same trend. This suggests that the rank order of
442 susceptibility of the species remains relatively constant across temperatures, but
443 as temperature increases the most susceptible species become more susceptible,
444 and the least susceptible less so.
445

446 Changes in global temperatures are widely predicted to alter host-parasite
447 interactions and therefore the likelihood of host shifts occurring [5,18,66–68]. The

448 outcome of these interactions may be difficult to predict if temperature causes a
449 different effect in the host and pathogen species [15,69–72]. Our results show that
450 changes in temperature may change the likelihood of pathogens jumping into
451 certain species, although they suggest that it may not alter which species are the
452 most susceptible to a novel pathogen.
453
454 The increase in phylogenetic variance with temperature is effectively a form of
455 genotype-by-environment interaction [25,73–75]. However, it varies from the
456 classically considered ecological crossing of reaction norms, as we do not see a
457 change in the rank order of species susceptibly. Instead, we find the species means
458 diverge with increasing temperatures and so the between species differences
459 increase [65,76].
460
461 As temperature is an important abiotic factor in many cellular and physiological
462 processes, we went on to examine the underlying basis of why viral load might
463 change with temperature. Previous studies that found phylogenetic signal in host
464 susceptibility were carried out at a single experimental temperature [34,35].
465 Therefore, the patterns observed could potentially be explained by some host
466 clades being assayed at sub-optimal thermal conditions. We used CT_{max} and CT_{min}
467 as proxies for thermal optima, which due to its multifaceted nature is problematic
468 to measure directly [77–79]. We also measured basal metabolic rate across three
469 temperatures to see if the changes in viral load could be explained by general
470 increases in enzymatic processes. We found that these measures were not
471 significant predictors of the change in viral load with temperature.
472

473 The host immune response and cellular components utilised by the virus are likely
474 to function most efficiently at the thermal optima of a species, and several studies
475 have demonstrated the outcomes of host-pathogen interactions can depend on
476 temperature [23,25,69,75]. However, the mechanisms underlying the changes in
477 susceptibility with temperature seen in this study are uncertain and a matter for
478 speculation. Our results show that in the most susceptible species, viral load
479 increases with temperature; this may be due to the virus being able to successful
480 infect and then freely proliferate, utilizing the host cells whist avoiding host
481 immune defences. In less susceptible species viral load does not increase with
482 temperature, and in some cases it actually appears to decreases. Here, temperature
483 may be driving an increase in biological processes such as enhanced host
484 immunity, or simply increasing the rate of degradation or clearance of virus
485 particles that have failed to establish an infection of host cells.
486
487 In conclusion, we have found changes in temperature can both increase or decrease
488 the likelihood of a host shift. Our results show the rank order of species
489 susceptibilities remain the same across temperatures, suggesting that studies of
490 host shifts at a single temperature can be informative in predicting which species
491 are the most vulnerable to a novel pathogen. Understanding how environmental
492 factors might affect broader taxonomic groups of hosts and pathogens requires
493 further study if we are to better understand host shifts in relation to climate change
494 in nature.
495

496 **Acknowledgements**

Many thanks to Darren Obbard and Frank Jiggins for useful discussion and Vanessa Kellerman and Johannes Overgaard for discussion about thermal assay methods. Thanks to Dave Hosken for use of BMR chambers and to the Drosophila Species Stock Centre for supplying flies.

References

1. Harvell CD, Mitchell CE, Ward JR, Altizer S, Dobson AP, Ostfeld RS, et al. Climate warming and disease risks for terrestrial and marine biota. Science. American Association for the Advancement of Science; 2002;296: 2158–62. doi:10.1126/science.1063699
2. Poulin R. Global warming and temperature-mediated increases in cercarial emergence in trematode parasites. Parasitology. Cambridge University Press; 2006;132: 143–151. doi:10.1017/S0031182005008693
3. Hoffmann AA, Sgrò CM. Climate change and evolutionary adaptation. Nature. Nature Publishing Group; 2011;470: 479–485. doi:10.1038/nature09670
4. Altizer S, Ostfeld RS, Johnson PTJ, Kutz S, Harvell CD. Climate change and infectious diseases: from evidence to a predictive framework. Science. 2013;341: 514–9. doi:10.1126/science.1239401
5. Redding DW, Moses LM, Cunningham AA, Wood J, Jones KE. Environmental-mechanistic modelling of the impact of global change on human zoonotic disease emergence: a case study of Lassa fever. Freckleton R, editor. Methods Ecol Evol. 2016;7: 646–655. doi:10.1111/2041-210X.12549
6. Mouritsen KN, Poulin R. Parasitism, climate oscillations and the structure of natural communities. Oikos. Munksgaard International Publishers; 2002;97: 462–468. doi:10.1034/j.1600-0706.2002.970318.x

7. Woolhouse MEJ, Haydon DT, Antia R. Emerging pathogens: the epidemiology and evolution of species jumps. Trends Ecol Evol. 2005;20: 238–44. doi:10.1016/j.tree.2005.02.009

8. Villordo SM, Filomatori C V, Sánchez-Vargas I, Blair CD, Gamarnik A V. Dengue Virus RNA Structure Specialization Facilitates Host Adaptation. Nagy PD, editor. PLoS Pathog. 2015;11: 1–22. doi:10.1371/journal.ppat.1004604

9. Musso D, Nilles EJ, Cao-Lormeau V-M. Rapid spread of emerging Zika virus in the Pacific area. Clin Microbiol Infect. 2014;20: O595–O596. doi:10.1111/1469-0691.12707

10. Leroy EM, Labouba I, Maganga GD, Berthet N. Ebola in West Africa: the outbreak able to change many things. Clin Microbiol Infect. 2014;20: O597–O599. doi:10.1111/1469-0691.12781

11. Caminade C, Kovats S, Rocklov J, Tompkins AM, Morse AP, Colón-González FJ, et al. Impact of climate change on global malaria distribution. Proc Natl Acad Sci U S A. National Academy of Sciences; 2014;111: 3286–91. doi:10.1073/pnas.1302089111

12. Tsetsarkin KA, Chen R, Leal G, Forrester N, Higgs S, Huang J, et al. Chikungunya virus emergence is constrained in Asia by lineage-specific adaptive landscapes. Proc Natl Acad Sci U S A. 2011;108: 7872–7877.

13. Messina JP, Brady OJ, Pigott DM, Golding N, Kraemer MUG, Scott TW, et al. The many projected futures of dengue. Nat Rev Microbiol. Nature Publishing Group; 2015;13: 230–239. doi:10.1038/nrmicro3430

14. Chen I-C, Hill JK, Ohlemüller R, Roy DB, Thomas CD. Rapid range shifts of species associated with high levels of climate warming. Science. American Association for the Advancement of Science; 2011;333: 1024–6.

547 doi:10.1126/science.1206432

548 15. Gehman A-LM, Hall RJ, Byers JE. Host and parasite thermal ecology jointly
549 determine the effect of climate warming on epidemic dynamics. Proc Natl
550 Acad Sci. 2018; 201705067. doi:10.1073/pnas.1705067115

551 16. Brooks DR, Hoberg EP. How will global climate change affect parasite-host
552 assemblages? Trends Parasitol. 2007;23: 571–574.
553 doi:10.1016/j.pt.2007.08.016

554 17. Brady OJ, Golding N, Pigott DM, Kraemer MUG, Messina JP, Reiner Jr RC, et al.
555 Global temperature constraints on Aedes aegypti and Ae. albopictus
556 persistence and competence for dengue virus transmission. Parasit Vectors.
557 BioMed Central; 2014;7: 338. doi:10.1186/1756-3305-7-338

558 18. Hoberg EP, Brooks DR. Evolution in action: climate change, biodiversity
559 dynamics and emerging infectious disease. Philos Trans R Soc Lond B Biol
560 Sci. The Royal Society; 2015;370: 20130553–20130553.
561 doi:10.1098/rstb.2013.0553

562 19. Thomas MB, Blanford S. Thermal biology in insect-parasite interactions.
563 Trends Ecol Evol. 2003;18: 344–350. doi:10.1016/S0169-5347(03)00069-7

564 20. Blanford S, Thomas MB. Host thermal biology: the key to understanding host-
565 pathogen interactions and microbial pest control? Agric For Entomol.
566 Blackwell Science Ltd; 1999;1: 195–202. doi:10.1046/j.1461-
567 9563.1999.00027.x

568 21. Labaude S, Moret Y, Cézilly F, Reuland C, Rigaud T, Ezilly FC, et al. Variation
569 in the immune state of Gammarus pulex (Crustacea, Amphipoda) according
570 to temperature: Are extreme temperatures a stress? Dev Comp Immunol.
571 2017;76: 25–33. doi:10.1016/j.dci.2017.05.013

572 22. Franke F, Armitage SAO, Kutzer MAM, Kurtz J, Scharsack JP. Environmental
573 temperature variation influences fitness trade-offs and tolerance in a fish-
574 tapeworm association. Parasit Vectors. BioMed Central; 2017;10: 252.
575 doi:10.1186/s13071-017-2192-7
576 23. Marshall ID. The influence of ambient temperature on the course of
577 myxomatosis in rabbits. J Hyg (Lond). 1959;57: 484–497.
578 doi:10.1017/S0022172400020325
579 24. Adamo SA, Lovett MME. Some like it hot: the effects of climate change on
580 reproduction, immune function and disease resistance in the cricket Gryllus
581 texensis. J Exp Biol. 2011;214: 1997–2004. doi:10.1242/jeb.056531
582 25. Mitchell SE, Rogers ES, Little TJ, Read AF. Host-Parasite and Genptype-By-
583 Environment Interactions : Temperature Modifies Potential For Selection By
584 a Sterilizing Pathogen. Evolution (N Y). 2005;59: 70–80.
585 doi:http://dx.doi.org/10.1554/04-526
586 26. Killen SS, Marras S, Metcalfe NB, McKenzie DJ, Domenici P. Environmental
587 stressors alter relationships between physiology and behaviour. Trends Ecol
588 Evol. Elsevier Ltd; 2013;28: 651–658. doi:10.1016/j.tree.2013.05.005
589 27. Kirk D, Jones N, Peacock S, Phillips J, Molnár PK, Krkošek M, et al. Empirical
590 evidence that metabolic theory describes the temperature dependency of
591 within-host parasite dynamics. Pawar S, editor. PLOS Biol. 2018;16:
592 e2004608. doi:10.1371/journal.pbio.2004608
593 28. Studer A, Thieltges DW, Poulin R. Parasites and global warming: Net effects
594 of temperature on an intertidal host-parasite system. Mar Ecol Prog Ser.
595 2010;415: 11–22. doi:10.3354/meps08742
596 29. Macnab V, Barber I. Some (worms) like it hot: fish parasites grow faster in

597 warmer water, and alter host thermal preferences. Glob Chang Biol. 2012;18:
598 1540–1548. doi:10.1111/j.1365-2486.2011.02595.x
599 30. Cable J, Barber I, Boag B, Ellison AR, Morgan ER, Murray K, et al. Global
600 change, parasite transmission and disease control: lessons from ecology.
601 Philos Trans R Soc B Biol Sci. The Royal Society; 2017;372: 20160088.
602 doi:10.1098/rstb.2016.0088
603 31. Gilbert GS, Webb CO. Phylogenetic signal in plant pathogen– host range. Proc
604 Natl Acad Sci U S A. 2007;104: 4979–4983. Available:
605 http://www.pnas.org/content/pnas/104/12/4979.full.pdf
606 32. de Vienne DM, Hood ME, Giraud T. Phylogenetic determinants of potential
607 host shifts in fungal pathogens. J Evol Biol. Blackwell Publishing Ltd;
608 2009;22: 2532–2541. doi:10.1111/j.1420-9101.2009.01878.x
609 33. Streicker DG, Turmelle AS, Vonhof MJ, Kuzmin I V, McCracken GF, Rupprecht
610 CE. Host phylogeny constrains cross-species emergence and establishment of
611 rabies virus in bats. Science. 2010;329: 676–9. doi:10.1126/science.1188836
612 34. Longdon B, Hadfield JD, Webster CL, Obbard DJ, Jiggins FM. Host phylogeny
613 determines viral persistence and replication in novel hosts. Schneider DS,
614 editor. PLoS Pathog. Elsevier Academic Press; 2011;7: e1002260.
615 doi:10.1371/journal.ppat.1002260
616 35. Longdon B, Hadfield JD, Day JP, Smith SCL, McGonigle JE, Cogni R, et al. The
617 causes and consequences of changes in virulence following pathogen host
618 shifts. Schneider DS, editor. PLoS Pathog. Public Library of Science; 2015;11:
619 e1004728. doi:10.1371/journal.ppat.1004728
620 36. Huey RB, Bennett AF. Phylogenetic studies of coadaptation:preferred
621 temperatures versus optimal performance temperature of lizards. Evolution

(N Y). 1987;41: 1098–1115.

37. Kellermann V, Loeschcke V, Hoffmann AA, Kristensen TN, Fløjgaard C, David JR, et al. Phylogenetic Constraints In Key Functional Traits Behind Species' Climate Niches: Patterns Of Desiccation And Cold Resistance Across 95 Drosophila Species. Evolution (N Y). 2012;66: 3377–89. doi:10.1111/j.1558-5646.2012.01685.x

38. Kellermann V, Overgaard J, Hoffmann AA, Flojgaard C, Svenning J-C, Loeschcke V. Upper thermal limits of Drosophila are linked to species distributions and strongly constrained phylogenetically. Proc Natl Acad Sci. National Academy of Sciences; 2012;109: 16228–16233. doi:10.1073/pnas.1207553109

39. Hoffmann AA, Chown SL, Clusella-Trullas S. Upper thermal limits in terrestrial ectotherms: how constrained are they? Fox C, editor. Funct Ecol. 2013;27: 934–949. doi:10.1111/j.1365-2435.2012.02036.x

40. Perlman SJ, Jaenike J. Infection Success in Novel Hosts : an Experimental and Phylogenetic Study of Drosophila -Parasitic Nematodes. Evolution (N Y). 2003;57: 544–557. doi:https://doi.org/10.1554/0014-3820(2003)057[0544:ISINHA]2.0.CO;2

41. Christian PD. Studies on Drosophila C and A viruses in Australian populations of Drosophila melanogaster. [Internet]. Australian National University. 1987. Available: http://hdl.handle.net/1885/142665

42. Webster CL, Waldron FM, Robertson S, Crowson D, Ferrari G, Quintana JF, et al. The discovery, distribution, and evolution of viruses associated with drosophila melanogaster. PLoS Biol. 2015;13: 1–33. doi:10.1371/journal.pbio.1002210

647 43. Webster CL, Longdon B, Lewis SH, Obbard DJ. Twenty-five new viruses
648 associated with the drosophilidae (Diptera). Evol Bioinforma. 2016;12: 13–
649 25. doi:10.4137/EBO.S39454
650 44. Arnold PA, Johnson KN, White CR. Physiological and metabolic consequences
651 of viral infection in Drosophila melanogaster. J Exp Biol. 2013;216: 3350–
652 3357. doi:10.1242/jeb.088138
653 45. Chtarbanova S, Lamiable O, Lee K-Z, Galiana D, Troxler L, Meignin C, et al.
654 Drosophila C virus systemic infection leads to intestinal obstruction. J Virol.
655 2014;88: 14057–69. doi:10.1128/JVI.02320-14
656 46. Johnson KN, Christian PD. The novel genome organization of the insect
657 picorna-like virus Drosophila C virus suggests this virus belongs to a
658 previously undescribed virus family. J Gen Virol. 1998;79: 191–203.
659 doi:10.1099/0022-1317-79-1-191
660 47. Ferreira ÁG, Naylor H, Esteves SS, Pais IS, Martins NE, Teixeira L. The Toll-
661 Dorsal Pathway Is Required for Resistance to Viral Oral Infection in
662 Drosophila. PLoS Pathog. 2014;10. doi:10.1371/journal.ppat.1004507
663 48. Jousset FX, Plus N, Croizier G, Thomas M. [Existence in Drosophila of 2
664 groups of picornavirus with different biological and serological properties]. C
665 R Acad Sci Hebd Seances Acad Sci D. 1972;275: 3043–6. Available:
666 http://www.ncbi.nlm.nih.gov/pubmed/4631976
667 49. Longdon B, Day JP, Alves JM, Smith SCL, Houslay TM, McGonigle JE, et al. Host
668 shifts result in parallel genetic changes when viruses evolve in closely
669 related species. PLoS Pathog. 2018;14: e1006951.
670 doi:10.1371/journal.ppat.1006951
671 50. Reed L, Muench H. A Simple Method of Estimating Fifty Per Cent Endpoints.

672 Am J Hyg. 1938;27: 231–239.

673 51. Lighton JRB. Measuring Metabolic Rates [Internet]. Measuring Metabolic
674 Rates: A Manual For Scientists. Oxford University Press; 2008.
675 doi:10.1093/acprof:oso/9780195310610.001.0001

676 52. Okada K, Pitchers WR, Sharma MD, Hunt J, Hosken DJ. Longevity, calling
677 effort, and metabolic rate in two populations of cricket. Behav Ecol Sociobiol.
678 2011;65: 1773–1778. doi:10.1007/s00265-011-1185-3

679 53. Arnqvist G, Dowling DK, Eady P, Gay L, Tregenza T, Tuda M, et al. Genetic
680 architecture of metabolic rate: environment specific epistasis between
681 mitochondrial and nuclear genes in an insect. Evolution. United States;
682 2010;64: 3354–3363. doi:10.1111/j.1558-5646.2010.01135.x

683 54. Huey RB, Moreteau B, Moreteau J-C, Gibert P, Gilchrist GW, Ives AR, et al.
684 Sexual size dimorphism in a Drosophila clade, the D. obscura group. Zoology.
685 2006;109: 318–330. doi:10.1016/j.zool.2006.04.003

686 55. Kearse M, Moir R, Wilson A, Stones-Havas S, Cheung M, Sturrock S, et al.
687 Geneious Basic: an integrated and extendable desktop software platform for
688 the organization and analysis of sequence data. Bioinformatics. 2012;28:
689 1647–1649.

690 56. Drummond A, Suchard M, Xi ED, Rambaut A. Bayesian phylogenetics with
691 BEAUti and the BEAST 1.7. Molecular Biology And Evolution 29; 2012.

692 57. Rambaut A, Suchard M, Xie D, Drummond A. Tracer v1.6. 2014. Available:
693 http://tree.bio.ed.ac.uk/software/tracer/

694 58. Rambaut A. FigTree [Internet]. 2006. Available:
695 http://tree.bio.ed.ac.uk/software/ figtree/.

696 59. Hadfield JD. MCMC methods for multi-respoinse generalized linear mixed

697 models: The MCMCglmm R package. J Stat Softw. 2010;33: 1–22.
698 doi:10.1002/ana.22635
699 60. R Development Core Team. R: A Language and Environment for Statistical
700 Computing. Vienna, Austria: R Foundation for Statistical Computing; 2005.
701 61. Housworth EA, Martins EP, Lynch M. The phylogenetic mixed model. Am Nat.
702 The University of Chicago Press; 2004;163: 84–96. doi:10.1086/380570
703 62. Felsenstein J. Maximum-likelihood estimation of evolutionary trees from
704 continuous characters. Am J Hum Genet. 1973;25: 471–492.
705 doi:10.1038/ncomms15810
706 63. Freckleton RP, Harvey PH, Pagel M. Phylogenetic analysis and comparative
707 data: a test and review of evidence. Am Nat. 2002;160: 712–26.
708 doi:10.1086/343873
709 64. Pagel M. Inferring the historical patterns of biological evolution. Nature.
710 1999;401: 877–884. doi:10.1038/44766
711 65. Ingleby FC, Hunt J, Hosken DJ. The role of genotype-by-environment
712 interactions in sexual selection. J Evol Biol. 2010;23: 2031–45.
713 doi:10.1111/j.1420-9101.2010.02080.x
714 66. Brooks DR, Hoberg EP. How will global climate change affect parasite–host
715 assemblages? Trends Parasitol. Elsevier Current Trends; 2007;23: 571–574.
716 doi:10.1016/J.PT.2007.08.016
717 67. Redding DW, Tiedt S, Lo Iacono G, Bett B, Jones KE. Spatial, seasonal and
718 climatic predictive models of Rift Valley fever disease across Africa. Philos
719 Trans R Soc B. 2017;372: 20160165.
720 doi:http://dx.doi.org/10.1098/rstb.2016.0165
721 68. Metcalf CJE, Walter KS, Wesolowski A, Buckee CO, Shevliakova E, Tatem AJ, et

722 al. Identifying climate drivers of infectious disease dynamics: recent
723 advances and challenges ahead. Proceedings Biol Sci. 2017;284: 20170901.
724 doi:10.1098/rspb.2017.0901
725 69. Murdock CC, Paaijmans KP, Bell AS, King JG, Hillyer JF, Read AF, et al.
726 Complex effects of temperature on mosquito immune function. Proceedings
727 Biol Sci. The Royal Society; 2012;279: 3357–66. doi:10.1098/rspb.2012.0638
728 70. Murdock CC, Paaijmans KP, Cox-Foster D, Read AF, Thomas MB. Rethinking
729 vector immunology: the role of environmental temperature in shaping
730 resistance. Nat Rev Microbiol. Nature Publishing Group; 2012;10: 869–876.
731 doi:10.1038/nrmicro2900
732 71. Nowakowski AJ, Whitfield SM, Eskew EA, Thompson ME, Rose JP, Caraballo
733 BL, et al. Infection risk decreases with increasing mismatch in host and
734 pathogen environmental tolerances. Ecol Lett. 2016;19: 1051–1061.
735 doi:10.1111/ele.12641
736 72. Cohen JM, Venesky MD, Sauer EL, Civitello DJ, McMahon TA, Roznik EA, et al.
737 The thermal mismatch hypothesis explains host susceptibility to an
738 emerging infectious disease. Ostfeld R, editor. Ecol Lett. 2017;20: 184–193.
739 doi:10.1111/ele.12720
740 73. Via S, Lande R. Genotype-Environment Interaction and the Evolution of
741 Phenotypic Plasticity. Evolution (N Y). 1985;39: 505–522.
742 74. Gomulkiewicz R, Kirkpatrick M. Quantitative Genetics and the Evolution of
743 Reaction Norms. Evolution (N Y). 1992;46: 390–411. doi:10.2307/2409860
744 75. Lazzaro BP, Flores HA, Lorigan JG, Yourth CP. Genotype-by-environment
745 interactions and adaptation to local temperature affect immunity and
746 fecundity in Drosophila melanogaster. PLoS Pathog. 2008;4: e1000025.

doi:10.1371/journal.ppat.1000025

76. Mitchell SE, Halves J, Lampert W. Coexistence of Similar Genotypes of Daphnia magna in Intermittent Populations : Response to Thermal Stress. Oikos. 2004;106: 469–478. doi:doi.org/10.1111/j.0030-1299.2004.13113.x

77. Chown SL, Jumbam KR, Sørensen JG, Terblanche JS. Phenotypic variance, plasticity and heritability estimates of critical thermal limits depend on methodological context. Funct Ecol. 2009;23: 133–140. doi:10.1111/j.1365-2435.2008.01481.x

78. Santos M, Castañeda LE, Rezende EL. Making sense of heat tolerance estimates in ectotherms: lessons from Drosophila. Funct Ecol. 2011;25: 1169–1180. doi:10.1111/j.1365-2435.2011.01908.x

79. Overgaard J, Kristensen TN, Sørensen JG. Validity of thermal ramping assays used to assess thermal tolerance in arthropods. PLoS One. 2012;7: 1–7. doi:10.1371/journal.pone.0032758

Supporting information

Supplementary methods: Set up and equipment for carrying out the CTmax/CTmin assays. Measurement correction model methods

S1 Table: Full list of species used in the experiment and their rearing food for stock populations.

S2 Table: Genbank accession numbers of sequences used to infer the host phylogeny.

772 **S1 Fig:** a) Viral load for 6 *Drosophilidae* species at 27°C, on day 0, day 1 and day 2
773 post infection. b) Change in viral load for the same 6 *Drosophilidae* species across
774 the three temperatures
775
776 **S2 Fig:** Ancestral state reconstructions of CT_{min} and CT_{max} for experimental flies.
777
778 **S3 Fig:** Change in Basal Metabolic Rate (BMR) for 44 *Drosophilidae* species across
779 three temperatures.
780
781 **S4 Fig:** Ancestral state reconstructions of BMR across the three experimental
782 temperatures

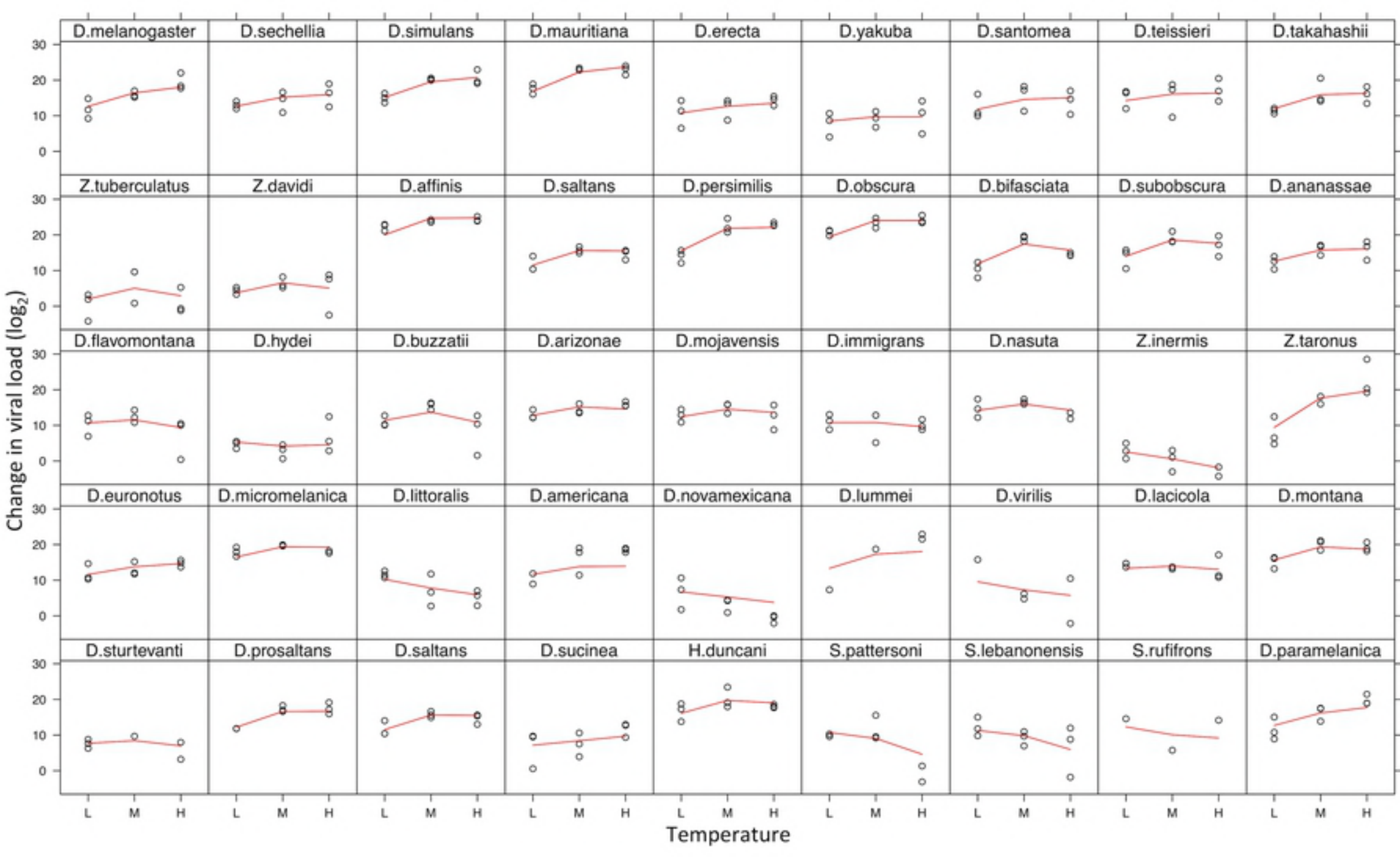
D.melanogaster
D.sechellia
D.simulans
D.mauritiana
D.erecta
D.yakuba
D.santomea
D.teissieri
D.takahashii
Z.tuberculatus
Z.davidi
D.affinis
D.saltans
D.persimilis
D.obscura
D.bifasciata
D.subobscura
D.ananassae
D.flavomontana
D.hydei
D.buzzatii
D.arizonae
D.mojavensis
D.immigrans
D.nasuta
Z.inermis
Z.taronus
D.euronotus
D.micromelanica
D.littoralis
D.americana
D.novamexicana
D.lummei
D.virilis
D.lacicola
D.montana
D.sturtevanti
D.prosaltans
D.saltans
D.sucinea
H.duncani
S.pattersoni
S.lebanonensis
S.rufifrons
D.paramelanica
Change in viral load (log2)
0
10
20
30
L
M
H
Temperature

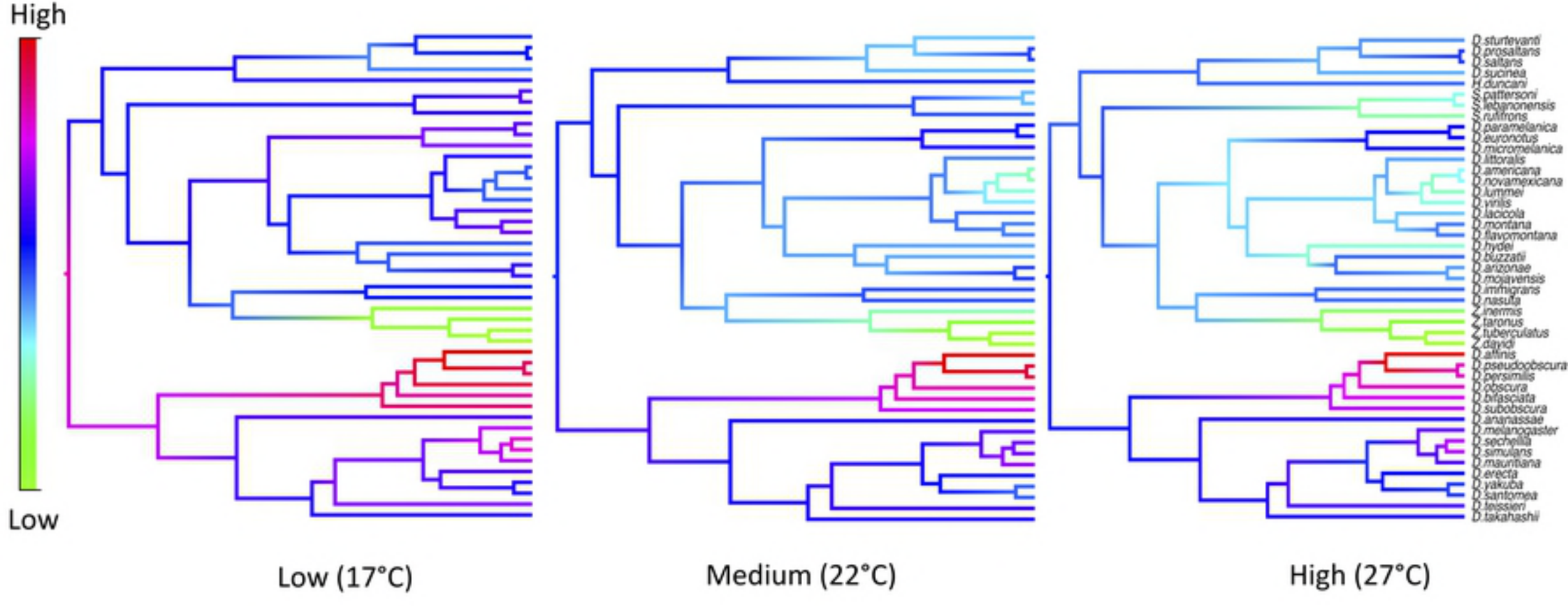
High
Low
D.sturtevanti
D.prosaltans
D.saltans
D.sucinea
H.duncani
S.pattersoni
S.lebanonensis
S.ruthrons
D.paramelanica
D.euronotus
D.micromelanica
D.littoralis
D.americana
D.novamexicana
D.lummei
D.virilis
D.lacicola
D.montana
D.flavomontana
D.hydei
D.buzzatii
D.arizonae
D.mojavensis
D.immigrans
D.nasuta
Z.inermis
Z.taronus
Z.tuberculatus
Z.davidi
D.affinis
D.pseudoobscura
D.persimilis
D.obscura
D.bifasciata
D.subobscura
D.ananassae
D.melanogaster
D.sechellia
D.simulans
D.mauritiana
D.erecta
D.yakuba
D.santomea
D.teissieri
D.takahashii
Low (17°C)
Medium (22°C)
High (27°C)